GRAPH LEARNING VIA SPECTRAL DENSIFICATION

Anonymous authors
Paper under double-blind review

ABSTRACT

Graph learning plays an important role in many data mining and machine learning tasks, such as manifold learning, data representation and analysis, dimensionality reduction, data clustering, and visualization, etc. For the first time, we present a highly-scalable spectral graph densification approach (GRASPEL) for graph learning from data. By limiting the precision matrix to be a graph-Laplacian-like matrix in graphical Lasso, our approach aims to learn ultra-sparse undirected graphs from potentially high-dimensional input data. A very unique property of the graphs learned by GRASPEL is that the spectral embedding (or approximate effective-resistance) distances on the graph will encode the similarities between the original input data points. By interleaving the latest high-performance nearly-linear time spectral methods, ultrasparse yet spectrally-robust graphs can be learned by identifying and including the most spectrally-critical edges into the graph. Compared with prior state-of-the-art graph learning approaches, GRASPEL is more scalable and allows substantially improving computing efficiency and solution quality of a variety of data mining and machine learning applications, such as manifold learning, spectral clustering (SC), and dimensionality reduction.

1 INTRODUCTION

Graph learning is playing increasingly important roles in many machine learning and data mining applications. For example, a key step of many existing machine learning methods requires converting potentially high-dimensional data sets into graph representations: it is a common practice to represent each (high-dimensional) data point as a node, and assign each edge a weight to encode the similarity between the two nodes (data points). The constructed graphs can be efficiently leveraged to represent the underlying structure of a data set or the relationship between data points (Jebara et al., 2009; Maier et al., 2009; Liu et al., 2018). However, how to learn meaningful graphs from large data set at scale still remains a challenging problem.

Several recent graph learning methods leverage emerging graph signal processing (GSP) techniques for estimating sparse graph Laplacians, which show very promising results (Dong et al., 2016; Egilmez et al., 2017; Dong et al., 2019; Kalofolias & Perraudin, 2019). For example, (Egilmez et al., 2017) addresses the graph learning problem by restricting the precision matrix to be a graph Laplacian and maximizing a posterior estimation of Gaussian Markov Random Field (GMRF), while an $l1$-regularization term is used to promote graph sparsity; (Rabbat, 2017) provides an error analysis for inferring sparse graphs from smooth signals; (Kalofolias & Perraudin, 2019) leverages approximate nearest-neighbor (ANN) graphs to reduce the number of variables for optimization. However, even the state-of-the-art Laplacian estimation methods for graph learning do not scale well for large data set due to their extremely high algorithm complexity. For example, solving the optimization problem for Laplacian estimation in (Dong et al., 2016; Kalofolias, 2016; Egilmez et al., 2017; Dong et al., 2019) requires $O(N^2)$ time complexity per iteration for N data entities and nontrivial parameters tuning for controlling graph sparsity which limits their applications to only very small data sets (e. g. with up to a few thousands of data points). The latest graph learning approach (Kalofolias & Perraudin, 2019) takes advantages of ANN graphs but can still run rather slowly for large data sets.

This work for the first time introduces a *spectral graph densification* approach (GRASPEL) for learning ultra-sparse graphs from data by leveraging the latest results in spectral graph theory (Feng, 2016; 2018; Zhao et al., 2018). GRASPEL has a close connection with prior GSP-based Laplacian estimation methods (Dong et al., 2016; Kalofolias, 2016; Egilmez et al., 2017; Kalofolias & Perraudin, 2019; Dong et al., 2019), and the graphical Lasso method (Friedman et al., 2008). By treating M-dimensional data points as M graph signals, GRASPEL allows efficiently solving a convex problem by iterative identifying and including the most spectrally-critical edges into the latest

graph leveraging recent nearly-linear time spectral methods (Feng, 2016; 2018; Zhao et al., 2018). Compared with prior spectral graph sparsification algorithms (Spielman & Srivastava, 2011; Feng, 2016) that aim to remove edges from a given graph while preserving key graph spectral properties, GRASPEL aims to add edges into the graph such that the learned graphs will have spectral embedding (or effective-resistance) distances encoding the distances between the original input data points. Comparing with state-of-the-art graph learning methods, GRASPEL is more scalable for estimation of attractive Gaussian Markov Random Fields (GMRFs) for even very large data set. We summarize the contribution of this work as follows:

• We propose a spectral graph densification approach (GRASPEL) that allows efficient estimation of attractive Gaussian Markov Random Fields (GMRFs) leveraging the latest spectral graph theory.

• We show that the graphical Lasso problem with a Laplacian-like precision matrix can be efficiently solved by including spectrally-critical edges to dramatically reduce spectral embedding distortions.

• The key to achieving high efficiency is a spectral embedding scheme for finding spectrally-critical edges, allowing each GRASPEL iteration to be completed in $O(N \log N)$ instead of $O(N^2)$ time.

• A novel convergence criterion has been introduced for terminating GRASPEL iterations based on graph spectral stability, or equivalently the signal smoothness across the leaned graphs.

• Our experiment results show that the graphs learned from high-dimensional data using GRASPEL can lead to more efficient and accurate spectral clustering (SC) as well as dimensionality reduction.

2 BACKGROUND OF GRAPH LEARNING VIA LAPLACIAN ESTIMATION

Given M observations on N data entities in a data matrix $X = [x_1, ..., x_M] \in \mathbb{R}^{N \times M}$, each column vector of X can be considered as a signal on a graph. The recent graph learning method (Dong et al., 2016) estimates graph Laplacians from X for achieving the following desired characteristics:

Smoothness of Graph Signals. The graph signals corresponding to the real-world data should be sufficiently smooth on the learned graph structure: the signal values will only change gradually across connected neighboring nodes. The smoothness of a signal x over a undirected graph $G = (V, E, w)$ can be measured with Laplacian quadratic form

$$x^\top Lx = \sum_{(p,q)\in E} w_{p,q}(x\,(p) - x\,(q))^2, \tag{1}$$

where $L = D - W$ denotes the Laplacian matrix of graph G with D and W denoting the degree and the weighted adjacency matrices of G, and $w_{p,q}$ denotes the weight for edge (p, q). The smaller value of (1) indicates the smoother signals across the graph. To quantify the smoothness (Q) of a set of signals X over graph G, the following matrix trace can be computed (Kalofolias, 2016):

$$Q(X, L) = Tr(X^\top LX), \tag{2}$$

where Tr denotes the matrix trace.

Sparsity of the Estimated Graph (Laplacian). Graph sparsity is another critical consideration in graph learning. One of the most important motivations of learning a graph is to use it for downstream data mining or machine learning tasks. Therefore, desired graph learning algorithms should allow better capturing and understanding the global structure (manifold) of the data set, while producing sufficiently sparse graphs that can be easily stored and efficiently manipulated in the downstream algorithms, such as graph clustering, partitioning, dimension reduction, data visualization, etc. To this end, the graphical Lasso algorithm (Friedman et al., 2008) has been proposed to learn the structure in an undirected Gaussian graphical model using $l1$ regularization to control the sparsity of the precision matrix. Given a sample covariance matrix S and a regularization parameter β, graphical Lasso targets the following convex optimization task:

$$\max_{\Theta} : \log\det(\Theta) - Tr(\Theta S) - \beta\|\Theta\|_1, \tag{3}$$

over all non-negative definite precision matrices Θ. The first two terms together can be interpreted as the log-likelihood under a Gaussian Markov Random Field (GMRF). $\|\cdot\|$ denotes the entry-wise $l1$ norm, so $\beta\|\Theta\|_1$ becomes the sparsity promoting regularization term. This model tries to learn the graph structure by maximizing the penalized log-likelihood. When the sample covariance matrix S is obtained from M i.i.d (independent and identically distributed) data points $X = [x_1, ..., x_M]$

where $X \sim N(0, S)$ has an N-dimensional Gaussian distribution with zero mean, each element in the precision matrix $\Theta_{i,j}$ encodes the conditional dependence between variables X_i and X_j. For example, $\Theta_{i,j} = 0$ implies that the corresponding variables X_i and X_j are conditionally independent, given the rest. However, the log-determinant problems are very computationally expensive. The emerging GSP-based methods infer the graph by adopting the criterion of signal smoothness (Kalofolias, 2016; Dong et al., 2016; Egilmez et al., 2017; Kalofolias & Perraudin, 2019). However, their extremely high complexities do not even allow for learning graphs with a few thousands of nodes . Furthermore, these methods require nontrivial parameters tuning for achieving good performance.

3 GRASPEL: GRAPH SPECTRAL LEARNING AT SCALE

At high level, GRASPEL gains insight from recent GSP-based Laplacian estimation methods (Dong et al., 2019), aiming to solve the following convex problem that is similar to the graphical Lasso problem (Friedman et al., 2008):

$$\max_{\Theta} : \log\det(\Theta) - \frac{1}{M} Tr(X^\top \Theta X) - \beta \|\Theta\|_1, \tag{4}$$

where $\Theta = L + \frac{I}{\sigma^2}$, L denotes the set of valid graph Laplacian matrices, I denotes the identity matrix, and $\sigma^2 > 0$ denotes prior feature variance. It can be shown that the three terms in (4) are corresponding to $\log\det(\Theta)$, $Tr(\Theta S)$ and $\beta\|\Theta\|_1$ in (3), respectively. When each column vector in the data matrix X [1] is treated as a graph signal vector, there is a close connection between our formulation and the graphical Lasso problem. Since $\Theta = L + \frac{I}{\sigma^2}$ correspond to symmetric and positive definite (PSD) matrices (or M matrices) with non-positive off-diagonal entries, this formulation will lead to the estimation of attractive GMRFs (Dong et al., 2019; Slawski & Hein, 2015). In case that X is non-Gaussian, (4) can be understood as Laplacian estimation based on minimizing the Bregman divergence between positive definite matrices induced by the function $\Theta \mapsto -\log\det(\Theta)$ (Slawski & Hein, 2015).

3.1 THEORETICAL BACKGROUND

Express the Laplacian matrix as

$$L = \sum_{(p,q)\in E} w_{p,q} e_{p,q} e_{p,q}^\top \tag{5}$$

where $e_p \in \mathbb{R}^N$ denotes the standard basis vector with all zero entries except for the p-th entry being 1, and $e_{p,q} = e_p - e_q$. Consider the objective function F in (4):

$$F = \log\det(\Theta) - \frac{1}{M} Tr(X^\top \Theta X) - \beta \|\Theta\|_1, \tag{6}$$

which can be further simplified as follows by substituting (5) into (6):

$$F = \sum_{i=1}^{N} \log(\lambda_i + 1/\sigma^2) - \frac{1}{M}\left(\frac{Tr(X^\top X)}{\sigma^2} + \sum_{(p,q)\in E} w_{p,q} \|X^\top e_{p,q}\|_2^2\right) - 4\beta \sum_{(p,q)\in E} w_{p,q}. \tag{7}$$

Taking the partial derivative with respect to the weight $w_{p,q}$ of edge (p, q) leads to:

$$\frac{\partial F}{\partial w_{p,q}} = \sum_{i=2}^{N} \frac{1}{\lambda_i + 1/\sigma^2} \frac{\partial \lambda_i}{\partial w_{p,q}} - \frac{1}{M} \|X^\top e_{p,q}\|_2^2 - 4\beta, \tag{8}$$

where the Laplacian eigenvectors corresponding to the ascending eigenvalues λ_i are denoted by u_i for $i = 1, ..., N$, satisfying:

$$L u_i = \lambda_i u_i. \tag{9}$$

According to the spectral perturbation analysis in Theorem 1 (Appendix), we have:

$$\frac{\partial \lambda_i}{\partial w_{p,q}} = \left(u_i^\top e_{p,q}\right)^2. \tag{10}$$

[1] For each of the original M-dimensional row vectors $X(i,:) \in \mathbb{R}^{1\times M}$ where $i = 1, ..., N$, the following pre-processing step will be performed: $X(i,:) = X(i,:) - \mu_i$, where μ_i denotes the sample mean of $X(i,:)$; as the result, the sample covariance matrix S in (3) becomes $\frac{XX^\top}{M}$.

Construct subspace matrices U_r and U_N for spectral graph embedding using the first $r-1$ and $N-1$ weighted nontrivial Laplacian eigenvectors, respectively:

$$U_r = \left[\frac{u_2}{\sqrt{\lambda_2 + 1/\sigma^2}}, ..., \frac{u_r}{\sqrt{\lambda_r + 1/\sigma^2}}\right], U_N = \left[\frac{u_2}{\sqrt{\lambda_2 + 1/\sigma^2}}, ..., \frac{u_N}{\sqrt{\lambda_N + 1/\sigma^2}}\right]. \tag{11}$$

Then (8) can be rewritten as:

$$\frac{\partial F}{\partial w_{p,q}} = \|U_N^\top e_{p,q}\|_2^2 - \frac{1}{M}\|X^\top e_{p,q}\|_2^2 - 4\beta \geq \|U_r^\top e_{p,q}\|_2^2 - \frac{1}{M}\|X^\top e_{p,q}\|_2^2 - 4\beta. \tag{12}$$

3.2 Graph Learning via Spectral Densification

Spectrally-critical edges. Define spectrally-critical edges to be the ones that can most effectively perturb the graph spectral properties, such as the first few Laplacian eigenvalues and eigenvectors. Then $\|U_r^\top e_{p,q}\|_2^2$ can be interpreted as the spectral sensitivity of the candidate edge (p, q): adding a candidate edge (p, q) with larger $\|U_r^\top e_{p,q}\|_2$ into the latest graph will more significantly perturb the first r Laplacian eigenvalues and eigenvectors. (12) implies that spectrally-critical edges will significantly impact the objective function (6) and have large *embedding distortions* defined as

$$\eta_{p,q} = \frac{M z_{p,q}^{emb}}{z_{p,q}^{data}}, \tag{13}$$

where $z_{p,q}^{emb} = \|U_N^\top e_{p,q}\|_2^2 \approx \|U_r^\top e_{p,q}\|_2^2$ and $z_{p,q}^{data} = \|X^\top e_{p,q}\|_2^2$ denote the ℓ_2 distances in the spectral embedding space and the original data vector space, respectively. Not surprisingly, as $\sigma^2 \to +\infty$ and $r \to N$, $z_{p,q}^{emb}$ becomes the effective-resistance distance, and $\eta_{p,q}$ becomes the edge leverage score for spectral graph sparsification (Spielman & Srivastava, 2011) when each edge weight is computed by $w_{p,q} = \frac{1}{z_{p,q}^{data}}$. Subsequently, (12) can be further simplified as follows:

$$\frac{\partial F}{\partial w_{p,q}} \approx \left(1 - \frac{1}{\eta_{p,q}}\right) z_{p,q}^{emb} - 4\beta, \tag{14}$$

implying that as long as $\eta_{p,q} > 1$ holds for the edge (p, q), the greater $\eta_{p,q}$ and $z_{p,q}^{emb}$ values will result in more significant improvement (increase) of the objective function.

Spectral graph densification. Prior research proves that for every undirected graph a nearly-linear-sized spectral sparsifier with $O(N \log N)$ edges can be computed in nearly-linear time by sampling each edge with a probability proportional to its leverage score (Spielman & Srivastava, 2011); on the contrary, the proposed GRASPEL framework can be considered as a spectral graph densification procedure that aims to identify and include the edges with large (effective-resistance) embedding distortions. Therefore, the graphical Lasso problem with Laplacian-like precision matrix can be efficiently solved via a spectral graph densification procedure that iteratively includes spectrally-critical edges into the latest graph so that the distortion in the graph spectral embedding space can be drastically mitigated. Consequently, a unique feature of GRASPEL is that the spectral embedding (effective-resistance) distances on the learned graph will encode the ℓ_2 distances between the original data points, which is key to many manifold learning and dimensionality reduction problems (Belkin & Niyogi, 2003; CAREY, 2017).

Convergence analysis. The global maximum can be achieved when (12) becomes zero. The convergence can be controlled by properly setting an embedding distortion threshold for η or sparsity constraint parameter β. When $\beta = 0$, the global maximum can be obtained when there exists no edge with $\eta > 1$ can be found for inclusion to the latest graph. Consequently, the convergence of GRASPEL iterations can be determined based on *graph spectral stability*: when the maximum embedding distortion η becomes small enough, or equivalently the first few Laplacian eigenvalues and eigenvectors become sufficiently stable, the GRASPEL iterations can be terminated. In comparison, choosing a proper β value for graphical Lasso can be very challenging in practical applications.

3.3 Overview of the GRASPEL Framework

Key steps in GRASPEL. Through the following steps, GRASPEL will iteratively identify and add the most spectrally-critical edges into the latest graph so that the spectral embedding distortion can be greatly mitigated, until no such edges can be found (as illustrated in Figure 1):

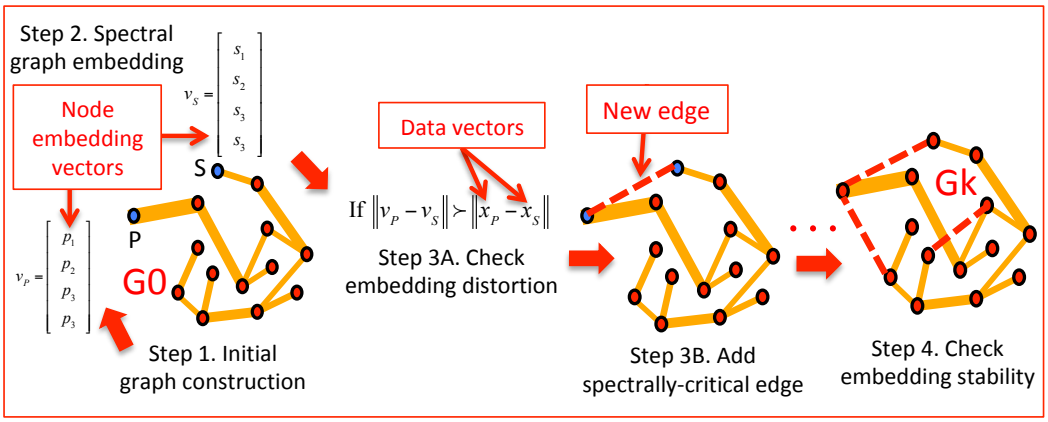

Figure 1: The overview of the proposed GRASPEL framework.

- **Step 1: Initial graph construction.** Similar to (Kalofolias & Perraudin, 2019), GRASPEL first constructs a sparse kNN graph that can be further sparsified leveraging scalable spectral sparsification algorithms (Spielman & Srivastava, 2011; Feng, 2018).
- **Step 2: Spectral graph embedding.** GRASPEL converts the latest graph into low-dimensional vector representations (e.g. v_s for node S in Figure 1) by exploiting a nearly-linear-time spectral graph embedding procedure (Zhao et al., 2018).
- **Step 3: Spectrally-critical edge identification.** By sorting nodes according to the Fiedler vector [2], GRASPEL efficiently identifies spectrally-critical edges with the greatest spectral embedding distortions, and subsequently includes them into the latest graph.
- **Step 4: Spectral stability checking.** The GRASPEL iterations will be terminated when the embedding distortions become sufficiently small, or equivalently when the graph spectra (e.g. the first few Laplacian eigenvalues and eigenvectors) become adequately stable.

Complexity analysis. Since each step in GRASPEL, such as kNN graph construction (Muja & Lowe, 2009; 2014; Malkov & Yashunin, 2018), spectral graph sparsification (Spielman & Srivastava, 2011; Feng, 2019) and embedding (Zhao et al., 2018), can be implemented based on nearly-linear $O(N \log N)$ time algorithms, each GRASPEL iteration can be completed in $O(N \log N)$ time, which is much faster than prior graph learning methods (Dong et al., 2016; Kalofolias, 2016; Egilmez et al., 2017; Dong et al., 2019) that require at least $O(N^2)$ time for each iteration.

4 Detailed Steps in GRASPEL

The detailed GRASPEL algorithm flow for graph learning has been described in Algorithm 1 in the Appendix. More details about each step in GRASPEL have been described as follows.

Step 1: Initial graph construction. As aforementioned, (approximate) kNN graphs can be constructed as the initial graph, since they can be obtained efficiently (Muja & Lowe, 2009), while being able to approximate the local data proximity (Roweis & Saul, 2000). However, the optimal k value (the number of nearest neighbors) is usually problem dependent and can be very difficult to find. In this work, GRASPEL will start with creating an (approximate) kNN graph using a relatively small k value (e.g. $k = 2$), which will suffice for approximating the local structure of the manifold, and strive to iteratively improve the approximation of the global manifold structure by adding a small portion of spectrally-critical edges through solving the proposed convex problem in (4). In addition, spectral sparsification (Spielman & Srivastava, 2011; Feng, 2019) can be leveraged to further simplify the initial kNN graph (Wang & Feng, 2017).

Step 2: Spectral graph embedding. Spectral graph embedding directly leverages the first few nontrivial eigenvectors for projecting nodes onto low-dimensional space (Belkin & Niyogi, 2003).

[2] The Laplacian eigenvector corresponding to the smallest nonzero eigenvalue.

The eigenvalue decomposition of Laplacian matrix is usually the computational bottleneck in spectral graph embedding, especially for large graphs (Shi & Malik, 2000; Von Luxburg, 2007; Chen et al., 2011). To achieve good scalability, nearly-linear time Laplacian solvers (Koutis et al., 2010) or multilevel Laplacian solvers (Zhao et al., 2018) can be exploited for much faster eigenvector (eigenvalue) computations without loss of accuracy.

Step 3: Spectrally-critical edge identification. Once Laplacian eigenvectors are available for the latest graph, through the following phases GRASPEL will identify spectrally-critical edges by looking at each candidate edge's embedding distortion defined in (13), while the following theorem can be derived for quantifying each candidate edge's impact on the first few Laplacian eigenvalues.

Theorem 1 *The spectral criticality $c_{p,q}$ of a candidate edge (p,q) considering the Laplacian eigenvalue λ_i can be estimated by $c_{p,q} = w_{p,q}\left(u_i^\top e_{p,q}\right)^2 \propto \eta_{p,q} = \frac{M z_{p,q}^{emb}}{z_{p,q}^{data}}$.*

Proof: See the Appendix.

Phase A: candidate edge identification with Fiedler vectors. Our approach for identifying spectrally-critical edges starts with sorting nodes according to the Fiedler vector that can be computed in nearly-linear time leveraging fast Laplacian solvers (Koutis et al., 2010; Spielman & Teng, 2014). This scheme is equivalent to including only the first nontrivial Laplacian eigenvector into U_r ($r = 1$) in (11) for spectral graph embedding. Subsequently, we can search candidate edge connections between the top and bottom few nodes in the 1D sorted node array. According to (14), only a small portion of node pairs with large embedding distances needs to be examined as candidate edges.

Phase B: embedding distortion estimation with multiple eigenvectors. With the first r Laplacian eigenvectors computed in the previous spectral embedding step, each node of the latest graph will be associated with an r-dimensional embedding vector, which allows the spectral embedding distortion of each candidate (spectrally-critical) edge to be quickly estimated. As discussed in Section 3.2, the spectral embedding distances computed with the first r eigenvectors can well approximate the effective-resistance distance thus the gradient in the proposed optimization task (8). Only the candidate edges with top embedding distortions will be added into the latest graph. Since the distances approximated using the first few eigenvectors will be the lower bounds of the effective-resistance distances, the lower bound of embedding distortions due to such an approximation can be estimated.

Step 4: Spectral stability checking. In this work, we propose to evaluate the edge embedding distortions with (13) for checking the spectral stability of the learned graph. If there exists no additional edge that has an embedding distortion greater than a given tolerance level (tol), GRASPEL iterations can be terminated. It should be noted that choosing different tolerance levels will result in graphs with different densities. For example, choosing a smaller distortion tolerance will require more edges to be included so that the resultant spectral embedding distances on the learned graph can more precisely encode the distances between the original data points. In practice, even for very large data set GRASPEL converges very quickly when starting with an initial 2NN or uNN (ultra-sparse nearest-neighbor) graph (Wang & Feng, 2017).

5 EXPERIMENTS

In this section, extensive experiments have been conducted to evaluate the performance of GRASPEL for a variety of public domain data sets (see the Appendix A.3 for detailed setting and evaluation metrics). In Sections A.6.1 and A.6.2 (see Appendix), we report additional experimental results for spectral clustering and dimensionality reduction (tSNE) applications leveraging the proposed GRASPEL approach. Since this work primarily focuses on learning graphs from high-dimensional data points, the proposed method can be orthogonal to existing research related to deep learning based spectral clustering methods: an autoencoder can be first applied to transform the input data into more optimal features that can subsequently become the input of GRASPEL for learning graphs in spectral clustering. For fair comparisons with other state-of-the-art graph learning methods, **we directly use the raw data as input without any additional pre-processing steps**.

5.1 EXPERIMENT SETUP

When applying Algorithm 1 to our data sets for the graph learning tasks shown in this section, we randomly sample candidate edges that connect between the top and bottom $0.05|V|$ ($\epsilon = 0.05$) nodes in the 1D sorted array according to the Fiedler vector, which allows GRASPEL to quickly

identify the most spectrally-critical edges; when estimating the spectral distortion of each candidate edge we compute the first $r = 2$ to 10 Laplacian eigenvectors for the spectral graph embedding step; we set the edge sampling ratio to be $\zeta = 0.001$ and add one edge ($s = 1$) to the latest graph in each GRASPEL iteration. $\sigma = 1E3$ in (11) has been used for computing Θ in all experiments. Clustering Accuracy (ACC) and Normalized Mutual Information (NMI) values (see definitions in the Appendix) are used for evaluating the spectral clustering results.

5.2 Experiment Results

Spectral stability checking. In Figure 2, we show how the objective function defined in (6) would change during the GRASPEL iterations when starting with **(a)** a 2NN graph, and **(b)** an ultra-sparse nearest neighbor (uNN) graph for the USPS data set. Only the first 50 Laplacian eigenvalues are computed for evaluating (6). The uNN graph is obtained by spectrally sparsifying a 5NN graph using the GRASS algorithm (with a relative condition number of 30) (Feng, 2019). We set the distortion tolerance to be $tol = 1$ for both cases and demonstrate the results for the first 30 GRASPEL iterations. As observed in Figure 2, **(a)** achieves a much greater objective function value after 30 iterations when comparing with **(b)**. Therefore, for very large data sets before going through the GRASPEL iterations a spectral sparsification procedure can be performed for further improving solution quality and runtime efficiency in graph learning. When starting with the 2NN graph, (6) grows rapidly within the first 10 iterations and much more slowly later on, which indicates the GRASPEL iterations have quickly converged [3]. We also show how the proposed scheme for spectral stability checking can be applied based on the embedding distortion metric defined in (13). GRASPEL iterations can be terminated when there exists no candidate edge that has a spectral embedding distortion greater than a given tolerance level (e.g. $\eta \geq tol$). As shown in Figure 2, for the USPS data set GRASPEL adds one additional edge in each iteration and requires only 11 iterations to effectively mitigate the maximum embedding distortion by over $2,600\times$.

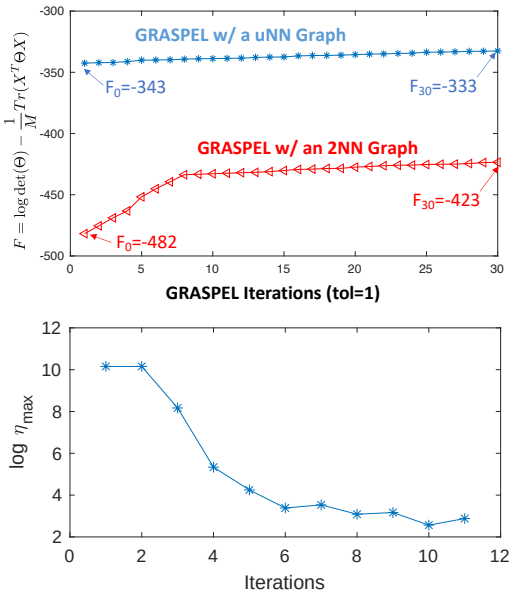

Figure 2: Objective function changes (top figure) and maximum spectral distortions (bottom figure) during GRASPEL iterations.

Spectral embedding results. In Figure 3, we show the first few Laplacian eigenvalues and 3D spectral drawings of the graphs learned with different distortion tolerance levels for a subset (including all the $24,462$ handwritten digits from 0 to 6) of the MNIST data set (see Appendix for details) and the test set of the Fashion MNIST dataset including $10,000$ article images from style 0 to 9 (Xiao et al., 2017). When creating the 3D spectral drawing layouts, each entry of the first three nontrivial Laplacian eigenvectors (u_2, u_3, u_4) corresponds to the x, y and z coordinates of each node (data point), respectively. The ground-truth label of each data point is shown using its corresponding color. The edges have been omitted in the graph layouts to better reveal the structure of the data points (manifolds).

Different embedding distortion tolerance levels are considered in our experiment. Starting from an initial 2NN graph, by adding one edge in each iteration GRASPEL has dramatically mitigated the spectral embedding distortions from by adding only a few additional edges into the initial 2NN graph. By examining the first few Laplacian eigenvalues, we notice that the initial 2NN graph of the MNIST data set has nine connected components (that equals the number of zero eigenvalues), while with 10 extra edges added via GRASPEL iterations, a well-connected graph can be formed for approximately preserving the structure of the original data set. For the MNIST data set we also observe relatively large gaps between the 6th and 7th eigenvalues, indicating that the intrinsic

[3] GRASPEL starts to experience negligible gradient values after 10 iterations and can not identify additional spectrally-critical candidate edges with large embedding distortions.

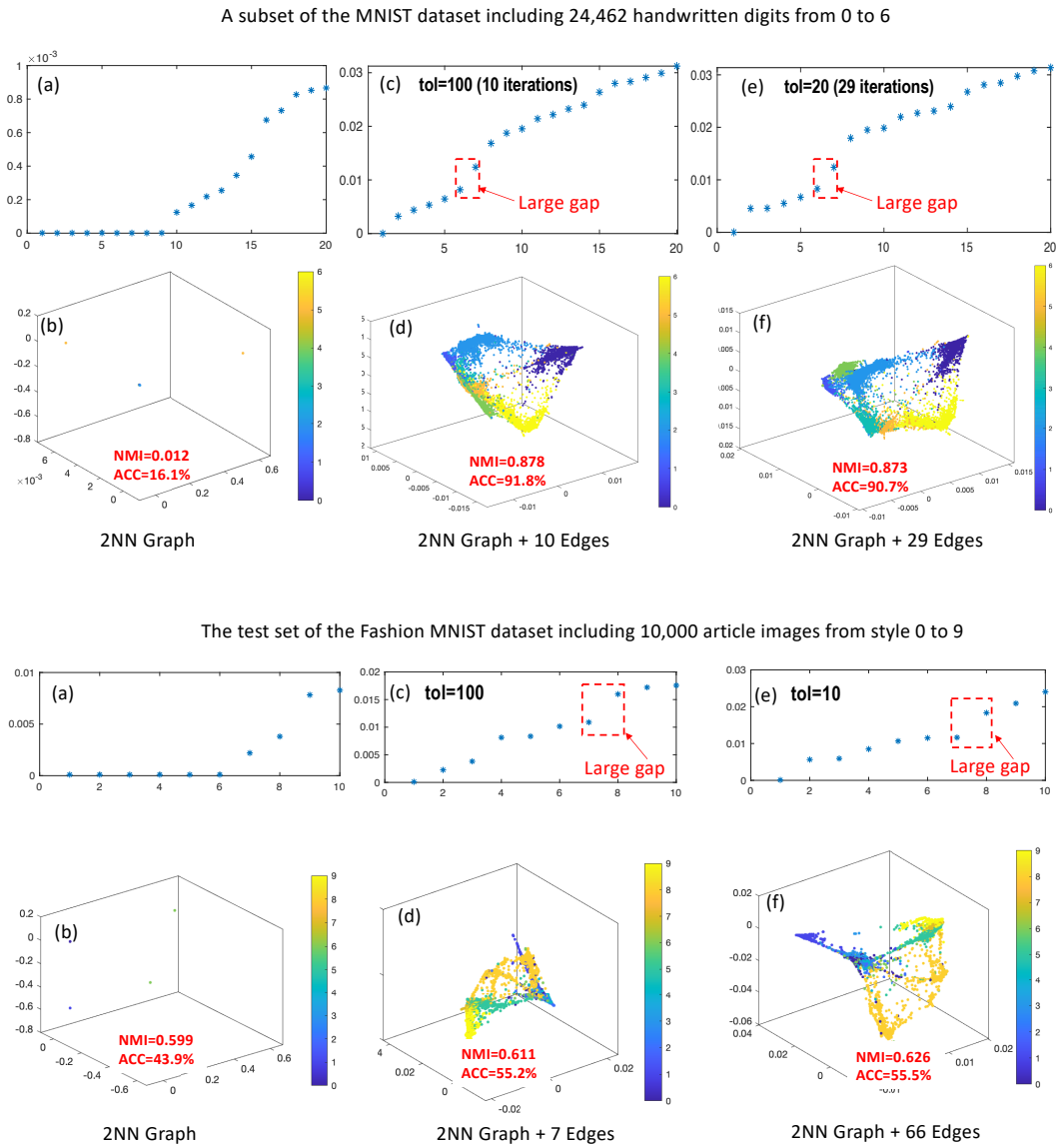

Figure 3: The first few Laplacian eigenvalues and 3D spectral drawings of the 2NN graph in figures (a) and (b), and the GRASPEL-learned graphs in figures (c) to (f).

dimensionality of the GRASPEL-learned graphs (manifolds) is approximately five, whereas for the Fashion MNIST data set the intrinsic dimensionality is approximately six.

6 Conclusion

In this work, we present a highly-scalable *spectral graph densification* approach (GRASPEL) for graph learning from data. By limiting the precision matrix to be a graph-Laplacian-like matrix in graphical Lasso, GRASPEL can always efficiently learns sparse undirected graphs from high-dimensional input data. A unique feature of the graphs learned by GRASPEL is that the effective-resistance distances will encode the similarities of the original data points. Compared with prior state-of-the-art graph learning approaches, GRASPEL is more scalable and always leads to substantially improved computing efficiency and solution quality for spectral clustering (SC) and dimensionality reduction tasks.

REFERENCES

Mikhail Belkin and Partha Niyogi. Laplacian eigenmaps for dimensionality reduction and data representation. *Neural computation*, 15(6):1373–1396, 2003.

CJ CAREY. *GRAPH CONSTRUCTION FOR MANIFOLD DISCOVERY*. PhD thesis, University of Massachusetts Amherst, 2017.

Wen-Yen Chen, Yangqiu Song, Hongjie Bai, Chih-Jen Lin, and Edward Y Chang. Parallel spectral clustering in distributed systems. *IEEE transactions on pattern analysis and machine intelligence*, 33(3):568–586, 2011.

Xiaowen Dong, Dorina Thanou, Pascal Frossard, and Pierre Vandergheynst. Learning laplacian matrix in smooth graph signal representations. *IEEE Transactions on Signal Processing*, 64(23): 6160–6173, 2016.

Xiaowen Dong, Dorina Thanou, Michael Rabbat, and Pascal Frossard. Learning graphs from data: A signal representation perspective. *IEEE Signal Processing Magazine*, 36(3):44–63, 2019.

Hilmi E Egilmez, Eduardo Pavez, and Antonio Ortega. Graph learning from data under laplacian and structural constraints. *IEEE Journal of Selected Topics in Signal Processing*, 11(6):825–841, 2017.

Zhuo Feng. Spectral graph sparsification in nearly-linear time leveraging efficient spectral perturbation analysis. In *Proceedings of the 53rd Annual Design Automation Conference*, pp. 57. ACM, 2016.

Zhuo Feng. Similarity-aware spectral sparsification by edge filtering. In *2018 55th ACM/ESDA/IEEE Design Automation Conference (DAC)*, pp. 1–6. IEEE, 2018.

Zhuo Feng. Grass: Graph spectral sparsification leveraging scalable spectral perturbation analysis. *arXiv preprint arXiv:1911.04382*, 2019.

Jerome Friedman, Trevor Hastie, and Robert Tibshirani. Sparse inverse covariance estimation with the graphical lasso. *Biostatistics*, 9(3):432–441, 2008.

Shivam Garg, Vatsal Sharan, Brian Zhang, and Gregory Valiant. A spectral view of adversarially robust features. In *Advances in Neural Information Processing Systems*, pp. 10138–10148, 2018.

Xiaojie Guo. Robust subspace segmentation by simultaneously learning data representations and their affinity matrix. In *IJCAI*, pp. 3547–3553, 2015.

Tony Jebara, Jun Wang, and Shih-Fu Chang. Graph construction and b-matching for semi-supervised learning. In *Proceedings of the 26th annual international conference on machine learning*, pp. 441–448. ACM, 2009.

Vassilis Kalofolias. How to learn a graph from smooth signals. In *Artificial Intelligence and Statistics*, pp. 920–929, 2016.

Vassilis Kalofolias and Nathanaël Perraudin. Large scale graph learning from smooth signals. *International Conference on Learning Representations (ICLR 2019)*, 2019.

I. Koutis, G. Miller, and R. Peng. Approaching Optimality for Solving SDD Linear Systems. In *Proc. IEEE FOCS*, pp. 235–244, 2010.

George C Linderman and Stefan Steinerberger. Clustering with t-sne, provably. *arXiv e-print, arXiv:1706.02582*, 2017.

Yang Liu, Quanxue Gao, Zhaohua Yang, and Shujian Wang. Learning with adaptive neighbors for image clustering. In *IJCAI*, pp. 2483–2489, 2018.

Laurens van der Maaten and Geoffrey Hinton. Visualizing Data using t-SNE. *Journal of machine learning research*, 9(Nov):2579–2605, 2008.

Markus Maier, Ulrike V Luxburg, and Matthias Hein. Influence of graph construction on graph-based clustering measures. In *Advances in neural information processing systems*, pp. 1025–1032, 2009.

Yury A Malkov and Dmitry A Yashunin. Efficient and robust approximate nearest neighbor search using hierarchical navigable small world graphs. *IEEE transactions on pattern analysis and machine intelligence*, 2018.

Marius Muja and David G Lowe. Fast approximate nearest neighbors with automatic algorithm configuration. *VISAPP (1)*, 2(331-340):2, 2009.

Marius Muja and David G Lowe. Scalable nearest neighbor algorithms for high dimensional data. *IEEE Transactions on Pattern Analysis and Machine Intelligence*, 36(11):2227–2240, 2014.

Christos H Papadimitrou and Kenneth Steiglitz. Combinatorial optimization: algorithms and complexity. 1982.

Vittal Premachandran and Ramakrishna Kakarala. Consensus of k-nns for robust neighborhood selection on graph-based manifolds. In *Proceedings of the IEEE Conference on Computer Vision and Pattern Recognition*, pp. 1594–1601, 2013.

Michael G Rabbat. Inferring sparse graphs from smooth signals with theoretical guarantees. In *2017 IEEE International Conference on Acoustics, Speech and Signal Processing (ICASSP)*, pp. 6533–6537. IEEE, 2017.

Sam T Roweis and Lawrence K Saul. Nonlinear dimensionality reduction by locally linear embedding. *science*, 290(5500):2323–2326, 2000.

Jianbo Shi and Jitendra Malik. Normalized cuts and image segmentation. *IEEE Transactions on pattern analysis and machine intelligence*, 22(8):888–905, 2000.

Martin Slawski and Matthias Hein. Estimation of positive definite m-matrices and structure learning for attractive gaussian markov random fields. *Linear Algebra and its Applications*, 473:145–179, 2015.

Daniel Spielman and Nikhil Srivastava. Graph Sparsification by Effective Resistances. *SIAM Journal on Computing*, 40(6):1913–1926, 2011.

Daniel A Spielman and Shang-Hua Teng. Nearly linear time algorithms for preconditioning and solving symmetric, diagonally dominant linear systems. *SIAM Journal on Matrix Analysis and Applications*, 35(3):835–885, 2014.

Alexander Strehl and Joydeep Ghosh. Cluster ensembles—a knowledge reuse framework for combining multiple partitions. *Journal of machine learning research*, 3(Dec):583–617, 2002.

Laurens Van Der Maaten. Accelerating t-SNE Using Tree-based Algorithms. *The Journal of Machine Learning Research*, 15(1):3221–3245, 2014.

Ulrike Von Luxburg. A tutorial on spectral clustering. *Statistics and computing*, 17(4):395–416, 2007.

Yongyu Wang and Zhuo Feng. Towards scalable spectral clustering via spectrum-preserving sparsification. *arXiv e-print, arXiv:1710.04584*, 2017.

Han Xiao, Kashif Rasul, and Roland Vollgraf. Fashion-mnist: a novel image dataset for benchmarking machine learning algorithms, 2017.

Zhiqiang Zhao, Yongyu Wang, and Zhuo Feng. Nearly-linear time spectral graph reduction for scalable graph partitioning and data visualization. *arXiv e-print, arXiv:1812.08942*, 2018.

A APPENDIX

A.1 PROOF OF THEOREM 1

Let $L \in \mathbb{R}^{N \times N}$ denote the Laplacian matrix of an undirected graph, and u_i denote the i-th eigenvector of L corresponding to the i-th eigenvalue λ_i that satisfies:

$$Lu_i = \lambda_i u_i, \tag{15}$$

then we have the following eigenvalue perturbation analysis:

$$(L + \delta L)(u_i + \delta u_i) = (\lambda_i + \delta\lambda_i)(u_i + \delta u_i), \tag{16}$$

where a perturbation $\delta L = \delta w_{p,q} e_{p,q} e_{p,q}^\top$ that implies a new edge connection is applied to L, resulting in perturbed eigenvalues and eigenvectors $\lambda_i + \delta\lambda_i$ and $u_i + \delta u_i$ for $i = 1, ..., N$, respectively.

Keeping only the first-order terms leads to:

$$L\delta u_i + \delta L u_i = \lambda_i \delta u_i + \delta\lambda_i u_i. \tag{17}$$

Write δu_i in terms of the original eigenvectors u_i for for $i = 1, ..., N$:

$$\delta u_i = \sum_{i=1}^{N} \alpha_i u_i. \tag{18}$$

Substituting (18) into (17) leads to:

$$L \sum_{i=1}^{N} \alpha_i u_i + \delta L u_i = \lambda_i \sum_{i=1}^{N} \alpha_i u_i + \delta\lambda_i u_i. \tag{19}$$

Multiplying $u_i^\top$ to both sides of (19) results in:

$$u_i^\top L \sum_{i=1}^{N} \alpha_i u_i + u_i^\top \delta L u_i = \lambda_i u_i^\top \sum_{i=1}^{N} \alpha_i u_i + \delta\lambda_i u_i^\top u_i. \tag{20}$$

Since u_i for for $i = 1, ..., N$ are unit-length, mutually-orthogonal eigenvectors, we have:

$$u_i^\top L \sum_{i=1}^{N} \alpha_i u_i = \alpha_i u_i^\top L u_i, \qquad \lambda_i u_i^\top \sum_{i=1}^{N} \alpha_i u_i = \alpha_i u_i^\top \lambda_i u_i. \tag{21}$$

Substituting (15) into (21), we have:

$$\alpha_i u_i^\top L u_i = \alpha_i u_i^\top \lambda_i u_i. \tag{22}$$

According to (21), we have:

$$u_i^\top \sum_{i=1}^{N} \alpha_i u_i = \lambda_i u_i^\top \sum_{i=1}^{N} \alpha_i u_i. \tag{23}$$

Substituting (23) into (20) leads to:

$$u_i^\top \delta L u_i = \delta\lambda_i u_i^\top u_i = \delta\lambda_i. \tag{24}$$

Then the eigenvalue perturbation due to δL is given by:

$$\delta\lambda_i = \delta w_{p,q} \left(u_i^\top e_{p,q}\right)^2. \tag{25}$$

Assume each edge weight is computed by $w_{p,q} = \frac{1}{z_{p,q}^{data}}$ where $z_{p,q}^{data} = \|X^\top e_{p,q}\|_2^2$. Since $\left(u_i^\top e_{p,q}\right)^2 \propto z_{p,q}^{emb} = \|U_N^\top e_{p,q}\|_2^2 \approx \|U_r^\top e_{p,q}\|_2^2$, as long as we can find an edge with large $w_{p,q}\left(u_i^\top e_{p,q}\right)^2$ or $\eta_{p,q} = \frac{M z_{p,q}^{emb}}{z_{p,q}^{data}}$, including this edge into the current graph will significantly perturb the Laplacian eigenvalue λ_i and eigenvector u_i. When $\sigma^2 \to +\infty$, the total (relative) spectral perturbation of the first r eigenvalues due to the inclusion of edge (p, q) becomes:

$$\Delta_r(e_{p,q}) = \sum_{i=2}^{r} \frac{\delta\lambda_i}{\lambda_i} = \delta w_{p,q} \|U_r^\top e_{p,q}\|_2^2. \tag{26}$$

A.2 Algorithm Flow

Algorithm 1 The GRASPEL Algorithm Flow

Input: A data matrix ($X = [x_1, ...x_M] \in \mathbb{R}^{N\times M}$) with N data points in M-dimensional, embedding distortion tolerance ($1 \leq tol$), window size for edge sampling ($0 < \epsilon \leq 50\%$), edge sampling ratio ($0 < \zeta \leq 1$), and the number of edges to be selected in each iteration ($0 < s$).
Output: The spectrally-learned graph G.

1: Construct an initial 2NN graph G using approximate kNN algorithms.
2: **while** $\eta_{max} \geq tol$ **do**
3: Embed the latest graph G using its Fiedler vector and sort the nodes into a 1D array I_{node};
4: Obtain node set N_{top} (N_{bot}) by including only the top (bottom) $\lceil \epsilon N \rceil$ nodes in I_{node};
5: Sample each of the $\lceil s/\zeta \rceil$ edges by randomly choosing one node from N_{top} and another node from N_{bot};
6: Form an edge set E_{sel} using edges with large distortions ($\eta \geq tol$) and set the largest edge embedding distortion as η_{max}.
7: **if** $|E_{sel}| \geq s$ **then**
8: Add the top s edges with largest η from E_{sel} into G;
9: **else**
Add all the edges in E_{sel} into G;
10: **end if**
11: **end while**
12: Return the learned graph G.

Algorithm 2 Spectral Clustering Algorithm

Input: A graph $G = (V, E, w)$ and the number of clusters r.
Output: Clusters $C_1...C_r$.

1: Compute the adjacency matrix A, and diagonal matrix D;
2: Obtain the unnormalized Laplacian matrix L=D-A;
3: Compute the eigenvectors u_1,...u_r that correspond to the bottom r nonzero eigenvalues of L;
4: Construct $U_r \in \mathbb{R}^{N\times r}$, with r eigenvectors of L stored as columns;
5: Perform k-means algorithm to partition the rows of U_r into r clusters and return the result.

A.3 Data Sets Description

COIL20: the data set contains $1,440$ gray-scale images of 20 objects, and each object on a turntable has 72 normalized gray-scale images taken from different degrees. The image size is 32x 32 pixels.

PenDigits: the data set consists of 7,494 images of handwritten digits from 44 writers, using the sampled coordination information. Each digit is represented by 16 attributes.

USPS: the data set includes $9,298$ scanned hand-written digits on the envelops from U.S. Postal Service with 256 attributes.

MNIST: the data set consists of 70,000 images of handwritten digits. Each image has 28-by-28 pixels in size. This database can be found at website (http://yann.lecun.com/exdb/mnist/).

A.4 COMPARED ALGORITHMS

Standard kNN: the most widely used affinity graph construction method. Each node is connected to its k nearest neighbors.

Consensus of kNN (cons-kNN) (Premachandran & Kakarala, 2013): adopts the state-of-the-art neighborhood selection methods to construct the affinity graphs. It selects strong neighborhoods to improve the robustness of the graph by using the consensus information from different neighborhoods in a given kNN graph.

LSGL (Kalofolias & Perraudin, 2019): a method to automatically select the parameters of the model introduced in (Kalofolias, 2016) given a desired graph sparsity level. The default settings have been used in our experiments.

A.5 EVALUATION METRIC

(1) **The ACC metric** measures the agreement between the clustering results generated by clustering algorithms and the ground-truth labels. A higher value of ACC indicates better clustering quality. The ACC can be computed by:

$$ACC = \frac{\sum_{j=1}^{n} \delta(y_i, map(c_i))}{n}, \tag{27}$$

where n is the number of samples in the data set, y_i is the ground-truth label provided by the data sets, and c_i is clustering result obtained from the algorithm. $\delta(x, y)$ is a delta function defined as: $\delta(x, y)$=1 for $x = y$, and $\delta(x, y)$=0, otherwise. $map(\bullet)$ is a permutation function that maps each cluster index c_i to a ground truth label, which can be realized using the Hungarian algorithm (Papadimitrou & Steiglitz, 1982).

(2) The NMI metric is in the range of [0, 1], while a higher NMI value indicates a better matching between the algorithm generated result and ground truth result. For two random variables P and Q, normalized mutual information is defined as (Strehl & Ghosh, 2002):

$$NMI = \frac{I(P, Q)}{\sqrt{H(P)H(Q)}}, \tag{28}$$

where $I(P, Q)$ denotes the mutual information between P and Q, while $H(P)$ and $H(Q)$ are entropies of P and Q. In practice, the NMI metric can be calculated as follows (Strehl & Ghosh, 2002):

$$NMI = \frac{\sum_{i=1}^{k}\sum_{j=1}^{k} n_{i,j} \log(\frac{n \cdot n_{i,j}}{n_i \cdot n_j})}{\sqrt{(\sum_{i=1}^{k} n_i \log \frac{n_i}{n})(\sum_{j=1}^{k} n_j \log \frac{n_j}{n})}}, \tag{29}$$

where n is the number of data points in the data set, k is the number of clusters, n_i is the number of data points in cluster C_i according to the clustering result generated by algorithm, n_j is the number of data points in class C_j according to the ground truth labels provided by the data set, and $n_{i,j}$ is the number of data points in cluster C_i according to the clustering result as well as in class C_j according to the ground truth labels.

A.6 ADDITIONAL EXPERIMENTAL RESULTS

A.6.1 GRAPH LEARNING FOR SPECTRAL CLUSTERING (SC)

The classical spectral clustering (SC) algorithm (see Algorithm 2 in the Appendix) first constructs a kNN graph where each edge weight encodes similarities between different data points (entities); then SC calculates the eigenvectors of the graph Laplacian matrix and embeds data points into low-dimensional space (Belkin & Niyogi, 2003); in the last, k-means algorithms are used to partition the data points into multiple clusters. The performance of SC strongly depends on the quality of the underlying graph (Guo, 2015). In this section, we apply GRASPEL for graph construction, and show the learned graphs can result in drastically improved efficiency and accuracy in SC tasks.

Table 1: Spectral Clustering Results

	ACC(%)/ NMI/ Time-C (seconds)/Time-S (seconds)			
Data Set	Standard KNN ($k = 10$)	ConskNN (Premachandran & Kakarala, 2013)	LSGL (Kalofolias & Perraudin, 2019)	GRASPEL
COIL-20	78.80/ 0.86/ **0.36**/0.37	79.86/ 0.86/ 0.54/0.28	65.48/0.77/60.22/1.02	**90.27/ 0.96/** 0.40/**0.19**
PenDigits	81.12/ 0.80/ **1.25**/0.47	84.17/ 0.81/ 8.59/46.41	75.01/0.72/1,622/15.64	**85.96/ 0.82/** 4.51/**0.27**
USPS	68.22/ 0.77/ **2.66**/1.02	78.94/ 0.82/ 19.82/74.57	72.35/0.71/2,598/29.37	**92.59/ 0.87/** 5.19/**0.21**
MNIST	71.95/ 0.72/ 242.38/6,785	-	-	**81.67/ 0.75/ 59.27/2.90**

- indicates that the method is not capable for handling data sets of this scale.

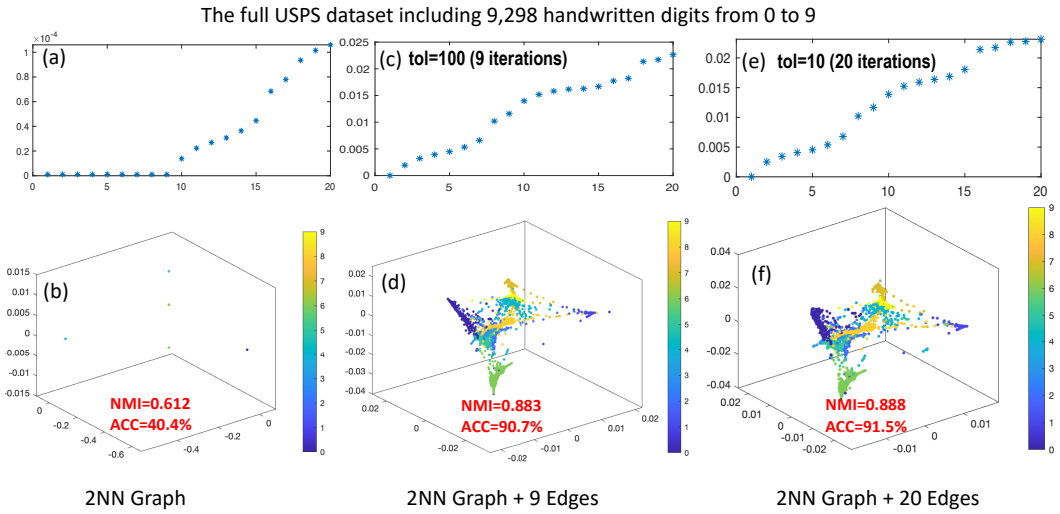

Figure 4: The first 20 Laplacian eigenvalues (top) and 3D spectral drawings (bottom) of the 2NN graph in figures (a) and (b), and the GRASPEL-learned graphs in figures (c) to (f).

Table 1 shows the ACC and NMI results of SC with graphs constructed by different methods with the best numbers highlighted, where graph construction time (Time-C) and spectral clustering time (Time-S) that involves eigendecomposition and kmeans clustering have also been reported. Note that the high computational and memory cost of recent GSP-based graph learning methods, such as GL-SigRep (Dong et al., 2016), GL-Logdet (Dong et al., 2016) and GLSC (Egilmez et al., 2017) do not allow for processing data sets with more than a few thousands data points, thus can not be used for real-world SC tasks. As observed, GRASPEL can consistently lead to dramatic performance improvement in SC, beating all competitors in clustering accuracy (ACC) across all data sets. Note that when starting with uNN graphs, the graphs learned by GRASPEL are ultra sparse, thereby allowing much faster eigendecompositions in SC when comparing with other methods (Wang & Feng, 2017): the SC of the MNIST data set with standard kNN ($k = 10$) takes over $6,000$ seconds, which will be dramatically improved to require less than three seconds (over $2,000X$ speedup) using the graph learned by our method (GRASPEL).

In Figures 4 and 5, additional SC results have been provided for the USPS and the Pendigit data sets by comparing two embedding distortion tolerance levels ($tol = 100$ and $tol = 10$). Not surprisingly, when starting with initial 2NN graphs a few GRASPEL iterations have already dramatically improved SC results: the normalized mutual information (NMI) has been improved from 0.612 to 0.888 for the USPS data set, and from 0.04 to 0.840 for the Pendigit data set; The spectral clustering accuracy (ACC) has been improved from 40.4% to 91.5% for the USPS data set, and from 15.2% to 89.4% for the Pendigit data set.

Since the number of zero Laplacian eigenvalues equals to the connected components in the learned graph, we observe that GRASPEL can always identify $O(q)$ spectrally-critical edges added to the initial 2NN graph so that its q connected components immediately get stitched into a connected graph for both test cases.

Discussion. The superior performance of GRASPEL is due to the following reasons: **1)** In traditional kNN graphs, all the nodes have the same degrees; as a result, the clustering may strongly favor balanced cut, which may lead to improper cuts in high-density regions of the graph. In con-

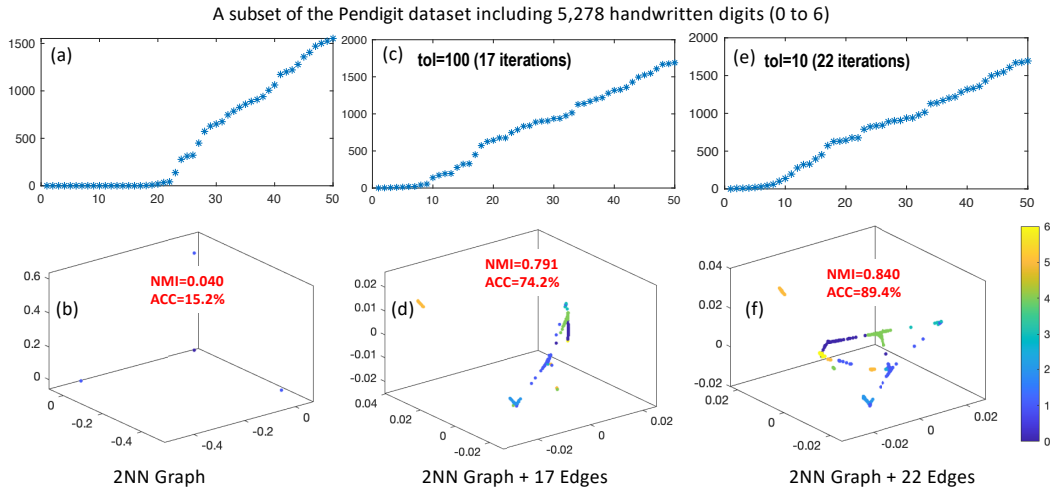

Figure 5: The first 50 Laplacian eigenvalues (top) and 3D spectral drawings (bottom) of the 2NN graph in figures (a) and (b), and the GRASPEL-learned graphs in figures (c) to (f).

trast, GRASPEL always learns ultra-sparse graphs that only include edges with the largest impact to graph spectral (structural) properties; as a result, the corresponding cuts will always occur in proper regions of the graph, which enables to handle even unbalanced data. **2)** Recent work (Garg et al., 2018) shows the fundamental connections between spectral properties of graphs associated with data and the inherent robustness to adversarial examples. Since GRASPEL identifies candidate edges by leveraging spectral graph properties, the learned graph structure will also be robust to input noises (perturbations).

A.6.2 Graph Learning for Dimensionality Reduction (DR)

The t-Distributed Stochastic Neighbor Embedding (t-SNE) has become one of the most popular visualization tools for high-dimensional data analytic tasks (Maaten & Hinton, 2008; Linderman & Steinerberger, 2017). However, its high computational cost limits its applicability to large scale problems. An substantially improved t-SNE algorithm has been introduced based on tree approximation (Van Der Maaten, 2014). However, for large data set the computational cost can still be very high.

A multilevel t-SNE algorithm has been proposed in (Zhao et al., 2018) leveraging spectral graph coarsening as a pre-processing step applied to the original kNN graph. A much smaller set of representative data points can be then selected from the coarsened graph for t-SNE visualization. In this work, we use GRASPEL to learn sparse graphs that can be further reduced into much smaller ones using spectral graph coarsening. Then more efficient t-SNE visualization can be achieved based on the sampled data points corresponding to the nodes in the coarsened graphs.

In our experiments, we first construct initial graphs by applying a spectral sparsification procedure to the 5NN graphs of both the MNIST and USPS data sets. Then a spectral graph coarsening procedure (Zhao et al., 2018) has been applied to create a hierarchy of coarse-level graphs. The t-SNE visualization can be obtained by directly using the data points corresponding to the nodes on the coarsest graph. Figure 6 shows the visualization and runtime results of the standard t-SNE (with tree-based acceleration) (Van Der Maaten, 2014) and the multilevel t-SNE algorithm (Zhao et al., 2018) based on graphs learned by GRASPEL. When using a $5X$ graph reduction ratio, t-SNE can be dramatically accelerated (12.8X and 7X speedups for MNIST and USPS data sets, respectively) without loss of visualization quality.

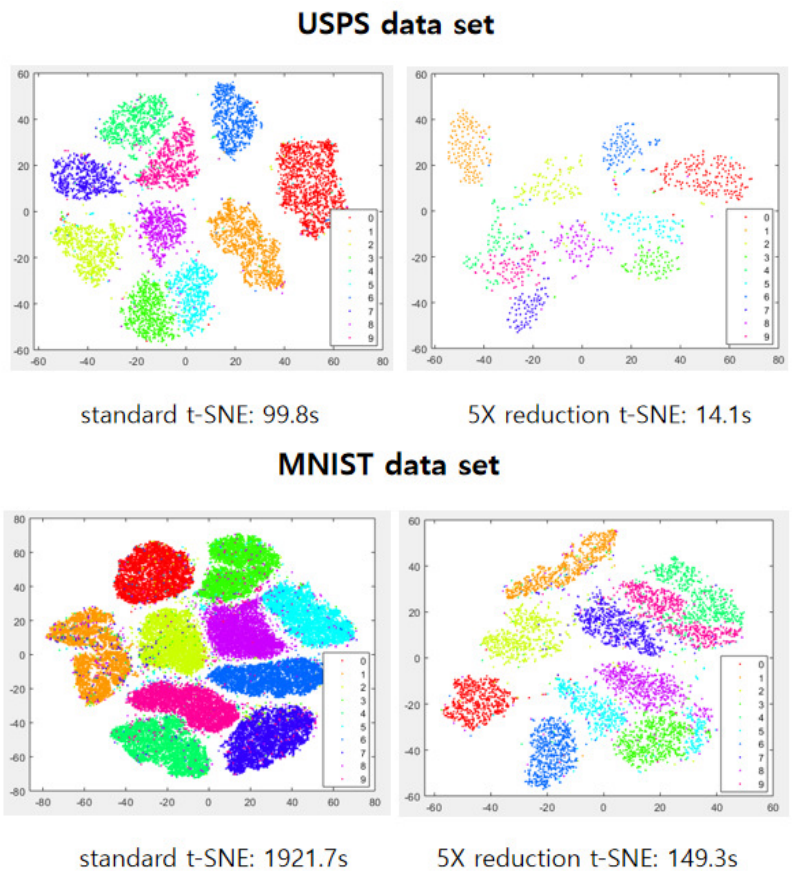

Figure 6: Multilevel t-SNE visualization results.